Journal of Ceramic Processing Research. Vol. 5, No. 1, pp. 48~52 (2004)

J O U R N A L O F
Ceramic Processing Research

High strain-to-failure porous alumina ceramics with improved mechanical properties

D. Doni Jayaseelan*, S. Ueno, T. Ohji and S. Kanzaki
Synergy Materials Research Center, National Institute of Advanced Industrial Science and Technology, Moriyama-ku, Nagoya - 463 8687, Japan

A pulse electric current sintering technique was employed to fabricate porous alumina from a commercially available powder. Porosity was controllable between 20 to 50% depending on the sintering temperature. The fracture strength was correlated exponentially as a function of porosity. A high strength of ~250 MPa was achieved for the specimens, which had porosity of 30 vol.%. The strain-to-failure of the porous Al_2O_3 ceramics increased considerably and this improves the reliability of the specimens.

Key words: porous material, ceramics, sintering, bending test, thermal stability.

Introduction

Porous ceramics find application in a variety of components including solid oxide fuel cell (SOFC) electrodes, battery separators, filters, catalyst supports, and preforms used to manufacture metal/ceramic composites by infiltration, etc. In cases where porous materials are used in harsh environments, an improvement in the mechanical properties is desirable because this is an important issue for increasing their reliability in practical applications. To improve the mechanical behavior of porous ceramic materials, various processing methods [1-7] were reported, but they could not simultaneously satisfy the requirements for porosity and strength of the materials, as they are frequently contradictory. Recently, we reported [8] a method to fabricate porous ceramics with high strength and high porosity. Although, there were many reports [9-12] on the effects of dopants on the properties of dense ceramics, there is no report available for porous ceramics. Similarly, the pulse electric current sintering (PECS) technique that has been widely used recently as an effective sintering technique for densifying poorly sinterable ceramic materials, and alloys, etc., has not been attempted for preparing porous ceramics [8, 13]. It is well known that PECS plays an important role in forming strong necks between grains at very low temperatures. In this study, we have carried out a series of experiments for many systems and the results are discussed in detail. In continuation to our previous work [8], two different secondary inclusions and two different dopants either by themselves or in combination were studied in order to prepare porous compacts. The present study substantiated the fact that the secondary inclusions and dopants are responsible for the grain boundary strengthening through strong necking.

*Corresponding author:
Tel : +81-52-739-0135
Fax: +81-52-739-0136
E-mail: daniel-doni@aist.go.jp

Experimental Details

The fabrication method of porous ceramics was reported earlier [8], which involves a combination of nanocomposite processing, doping, and pulse electric current sintering. High purity α-Al_2O_3 powder with a mean particle size of 0.21 μm (Taimicron TM-DAR, TKK, Japan) was used as the starting material. β-SiC (Ibiden Co., Japan) and 3Y.ZrO_2 (Tosoh Co., Japan) were used as the secondary phases and nitrate salt of Mg, and TiO_2 were used as the dopants. The powders were wet ball mixed in the correct ratio (Al_2O_3 (100 ppm MgO)/3 vol.% ZrO_2, AZM; Al_2O_3 (100 ppm MgO, 500 ppm TiO_2,)/3 vol.% ZrO_2, AZTM; and Al_2O_3/5 vol.% SiC, AS), in a polyethylene jar for 24 hours in an ethanol medium using high purity alumina balls. The respective designations will be used throughout the text hereafter. All compositions were densified by the PECS technique at different temperatures and the experimental conditions were given previously [8]. Density measurements were carried out by the Archimedes method using water as the medium. Pore size distribution was determined by mercury porosimetry (Autopore 9220, Shimadzu Corp., Japan). Rectangular bars of dimensions 3 mm × 2 mm × 23 mm were machined from the sintered disks. The flexural strength at room temperature was determined using a three-point bend test with a span of 16 mm with a crosshead speed of 0.5 mm/minute. Young's moduli were determined by

the pulse-echo method according to JIS 1602 and the data for Young's moduli represents the average of three samples. The pore structures of the porous support were observed by scanning electron microscopy (SEM). The grain size was measured by the linear intercept method.

Results and Discussion

Fabrication of porous ceramics

Alumina (hereafter will be referred as Al), AS, AZM and AZTM with different levels of porosity were fabricated by the PECS technique. Initially, trial experiments were conducted to optimize the sintering parameters. Porosity was controllable between 20~50% depending on the sintering temperature. Figure 1 shows the relative density of the specimens as a function of sintering temperature. A conceptual model for the sintering behavior of alumina has been realized based on the experimental results of the present study (Fig. 1). As in any sintering processes, PECS starts with a highly porous body. The plateau between 900 and 1050 °C, seen in Fig. 1, corresponds to the rearrangement of particles with initial formation of necks. Particle rearrangement in the initial stage of sintering is one of the notable mechanisms in porous ceramics as agglomerates can cause differential sintering and lead to fissures in microstructures, creating potential origins of fracture. This rearrangement is usually influenced by either applied pressure and/or temperature in the early stage of sintering, which is lacking in the case of conventional pressureless sintering. The neck formation is due to the geometric amplification of pressure on the interparticle point contacts, but as the neck grows, the local pressure at the neck is substantially reduced.

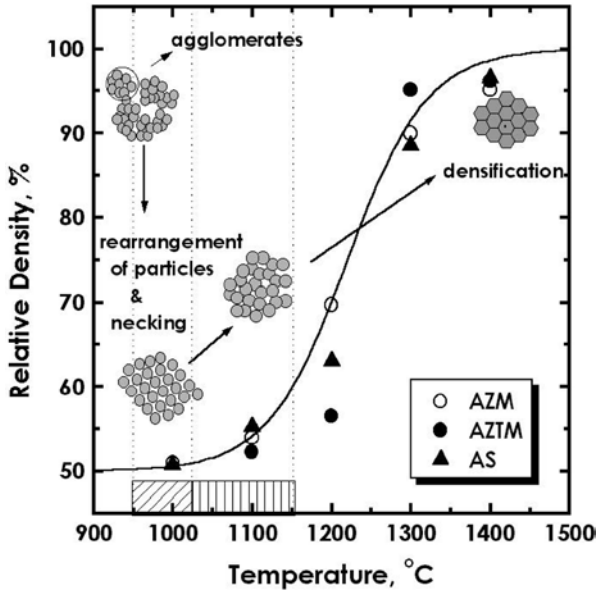

Fig. 1. The densification behavior of porous alumina ceramics as a function of sintering temperature.

However, in the case of the PECS process it has been suggested that the pulsed current can make a major contribution to densification during the initial part of a sintering process. This stage occurs in present case between 1050°C and 1150°C, which involves very little shrinkage. At these temperatures, surface diffusion is more dominant than volume diffusion, thereby increasing the size of neck growth. This stage is exactly the transition from surface diffusion to the initial stage of grain boundary diffusion. After particles have become connected together, second stage starts; diffusion process is the main contributor for the densification at this stage. The highest temperature achieved in necks provides the highest diffusion rate and thus enhances matter transport towards the neck area. It should be noted that the linear change in shrinkage can be monitored and because of this, we can avoid later stage of sintering by interrupting the heating schedule.

Mechanical properties

The characteristic results of the mechanical properties for different alumina-based porous specimens are summarized in Table 1. As a generic character, the porosity of the intergranular alumina compacts mainly depends on the sintering temperature. The fracture

Table 1. Mechanical properties of porous ceramics

Material	Open Porosity %	Strength MPa	Modulus GPa	Poisson's Ratio
pure alumina	56	37 ± 3	-	-
(pressureless	50	49 ± 5	-	-
sintering)	41	71 ± 4	57	-
	35	92 ± 7	95	-
	29	123 ± 12	167	-
	20	212 ± 13	208	-
pure alumina	49	70 ± 2	65	0.225
(PECS)	42	92 ± 2	71	0.228
	32	173 ± 6	167	0.231
	24	252 ± 8	173	0.235
AS (PECS)	55	65 ± 2	-	
	50	86 ± 2	-	
	45	112 ± 5	78	0.216
	38	184 ± 7	93	0.235
	33	213 ± 12	-	-
	31	261 ± 13	170.3	0.2
AZM (PECS)	49	101 ± 3	27	0.216
	45	113 ± 5	48	0.216
	38	154 ± 5		
	30	251 ± 8	76	0.212
AZTM (PECS)	50	107 ± 5	32	0.219
	44	154 ± 7	-	
	39	192 ± 8	62	0.221
	35	221 ± 11	-	
	32	272 ± 13	71	0.222

strength and the Young's modulus strongly depend on porosity. However, the poisson's ratio seems to be not affected much by porosity, though there is little variation. In contrast to low strength values for porous alumina fabricated by either hot pressing or pressureless sintering in earlier studies, [2-4] our present study shows a better increase in strength (Table 1). This increase in strength must be attributed to necking and strong interface bonding between alumina grains. [8] When 5 vol.% of SiC was added as a secondary phase, the fracture strength increased to ~250 MPa for specimens having porosity of 30%. Similarly, when alumina was added with 3 vol.% 3Y-TZP, and doped with MgO and TiO_2, the fracture strength improved further (> 250 MPa). Although, secondary inclusions and dopants aid for an improvement of fracture strength, they did not affect the Young's modulus of the specimens, so that the strain to failure of these specimens was much higher.

The flexural strength of the porous alumina has been fitted based on the least square method [16] and is shown in Fig. 2a. Good correlation coefficient (R^2) was obtained for all compositions and this high correlation factor indicates that the porosity-strength behavior of porous alumina could be well described by an exponential function. The values of fracture strength extrapolated at P=0 by the fitted equation are typical values observed for alumina based ceramics. The consistency in *b* value obtained in the present study for the PECSed samples (Table 2) indicates a non-dependent nature of the pore structure with the secondary inclusions and dopants. This ensures that the secondary inclusions and dopants do not alter the pore structure as shown in Fig. 3, which is otherwise necessary in optimizing microstructural design.

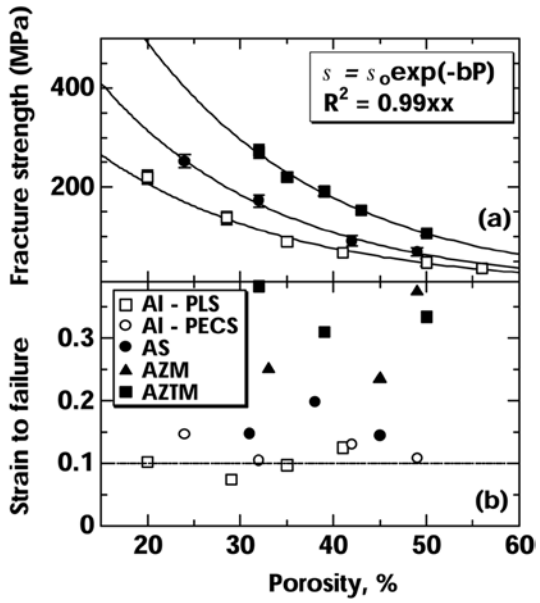

Fig. 2. Mechanical properties of alumina-based porous ceramics (a) A least square fit of exponential curve of fracture strength of alumina-based ceramics as a function of porosity (b) Strain to failure of alumina-based ceramics as a function of porosity.

Table 2. Parameters of an exponent fit performed on fracture strength for the porosity range 20-50 vol.%.

Sample	Extrapolated value at P=0	*b*	Correlation coefficient (R^2)
Al-PLS	499	4.7	0.9924
Al-PECS	904	5.29	0.9934
AS-PECS	1425	5.64	0.9934
AZTM-PECS	1350	5.06	0.9954

PLS-pressureless sintering; PECS-pulse electric current sintering.

Based on crack-microstructure interaction, as the fracture mode was preferentially intergranular; the strength of porous alumina ceramics in this study can also be related to the minimum solid contact area. Therefore, the bonding interface could be viewed as the minimum solid contact area. The nominal interface bonding strength can be evaluated by [17],

$$\sigma_{bonding} = E_o \varepsilon_f \quad (1)$$

where E_o is the Young's modulus and ε_f is the strain-to-failure of porous alumina. The values of strain-to-failure of porous alumina ceramics are plotted against the volume fraction of porosity, as shown in Fig. 2b. In general, stronger grain bonding in porous alumina can be due to the homogeneous microstructure of compacts prepared by the compaction pressure during sintering. The characteristic values of strain-to-failure for different porous alumina- based ceramics imply that strong necks have formed between the grains. The interfacial bonding strength seems to depend on the starting composition. In the case of pressureless sintering, the localized non-uniform shrinkage in the compact during sintering causes a localized non-uniform strain inside and at the edges of the grains. This would result in a number of defects at the grain boundaries connecting the grains and lead to a weak interfacial bonding. This is overcome by means of PECS. It is observed that monolithic porous alumina sintered by PECS had a slightly large strain-to-failure than that sintered by pressureless sintering. Above all, AS and AZTM porous compacts exhibited further high strain-to-failure. It is a clearly evident that the secondary inclusions and dopants improved the mechanical properties of porous ceramics via grain bonding strengthening. This is because the segregation of minor elements to the grain boundaries could alter the grain boundary fracture resistance [18-20]. Hence, it can be realized that the role of the sintering additive is not just to promote densification but also to affect the grain boundary resistance by changing the interfacial energy, as the type of dopant changes the surface energy and grain boundary energy. The origin of the change in grain boundary fracture energy seems to be associated with the segregated

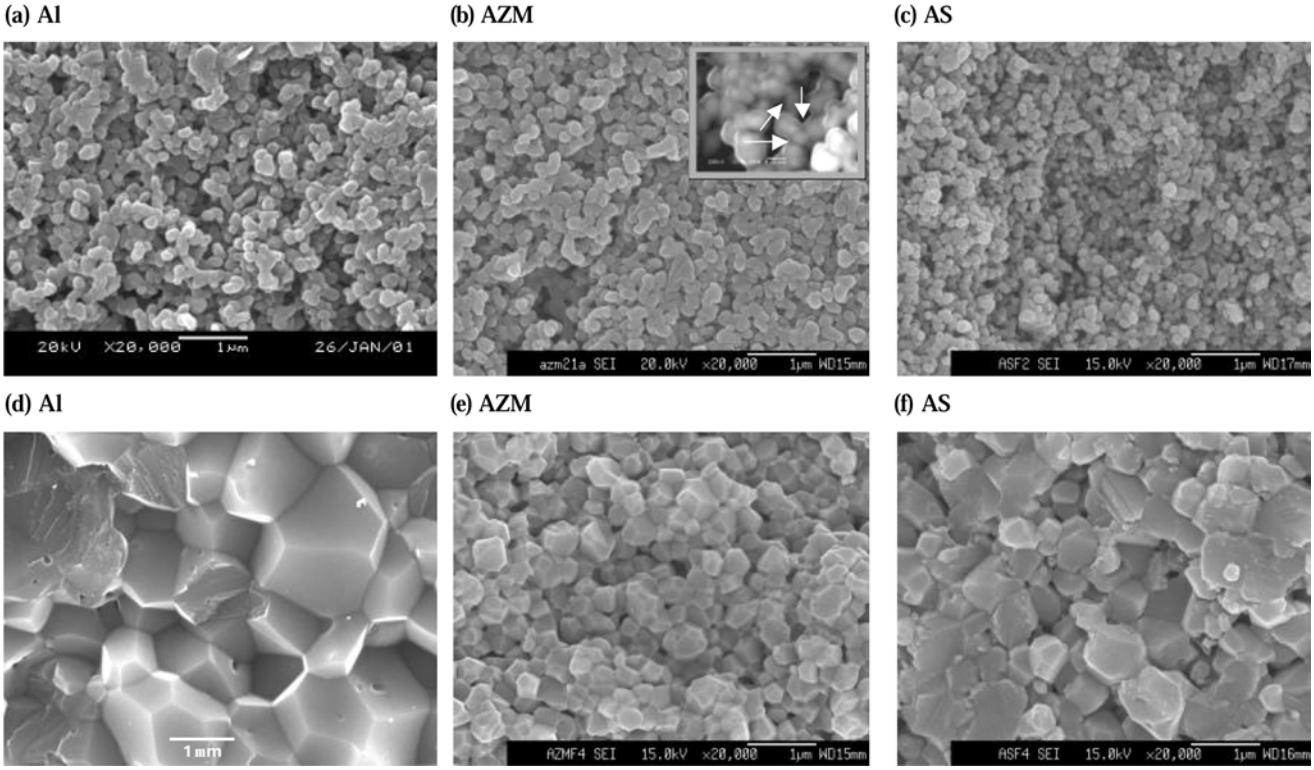

Fig. 3. (a)-(c) Morphology of alumina grains of porous compacts sintered at 1200°C (c)-(f) Fracture surface of dense alumina compacts sintered at 1400°C.

cations in grain boundaries. Therefore, the formation of an appropriately strong 'bridge' is a decisive first for the mechanical strength and chemical resistance of a given material, affecting also such parameters as flow resistance of liquids and gases, gas hold up, etc [19, 20]. The characteristic values of strain-to-failure for different porous alumina ceramics imply that strong necks have formed between the grains. The interfacial bonding strength depends on the composition of the starting material.

Microstructure

Figure 3 shows the microstructures of alumina specimens. Figures 3a-3c represent the grain morphology of porous alumina ceramics, whereas Figs. 3d-3f represent the fractured surface of dense compacts of respective specimens. The noted microstructural characteristics of porous compacts include matrix grain size and neck size between the particles. It is also noted that the increased contact area between grains occurring during PECS, results in enhanced necks and improvements in material strength with little loss in open porosity. The size of alumina grains of the porous compacts when sintered at 1200°C is measured to be 200 nm, which is the same as that of the starting material and the median pore size is measured to be ~75 nm (not shown here). That is, no grain growth occurred in the specimens. When we look at the grain morphology of porous compacts, it remains the same for all compositions. In other words, the secondary inclusions and dopants did not alter the morphology of grains in the porous compacts (Figs. 3a-3c). However, this is not the case in the dense microstructure (Figs. 3d-3e). The compacts when the appropriate secondary inclusions and/or dopants were added, had constrained grains with homogeneous microstructures and indeed they differ from each other. Monolithic alumina had larger grains, whereas the secondary inclusions considerably restrained the grain growth.

Summary

In the present study, a series of porous alumina ceramics were fabricated by a Pulse Electric Current Sintering method. The effect of nano-composite processing and doping improved the grain bonding between grains. Simultaneously, the discharges associated during the PECS process, greatly assisted for the initial formation of strong necks between grains. A high strain-to-failure demonstrates that the addition of secondary inclusions and dopants significantly improved the mechanical properties of the porous ceramics through the formation of strong necks. Therefore, porous materials fabricated by this method with high mechanical strength can be used in harsh environments, such as high-pressure filters.

Acknowlegements

This work has been supported by METI, Japan, as

part of the Synergy Ceramics Project. The authors are members of the Joint Research Consortium of Synergy Ceramics.

References

1. K. Ishizaki, S. Komarneni, and M. Nanko, Porous Materials: Process technology and applications, Materials Technology Series, Kluwer Academic Publishers; 1998; p.56-65.
2. D.C.C. Lam, F.F. Lange, and A.G. Evans, J. Am. Ceram. Soc. 77 (1994) 2113-2117.
3. S.C. Nanjangud, R. Brezny, and D.J. Green, J. Am. Ceram. Soc. 78 (1995) 266-268.
4. T. Ostrowski, and J. Rodel, J. Am. Ceram. Soc. 82 (1999) 3080-3086.
5. Y. Shigegaki, M.E. Brito, K. Hirao, M. Toriyama, and S. Kanzaki, J. Am. Ceram. Soc. 80 (1997) 495-498.
6. N. Kondo, Y. Suzuki, and T. Ohji, J. Mat. Res. 16 (2001) 32-34.
7. T. Fukasawa, M. Ando, T. Ohji, and S. Kanzaki, J. Am. Ceram. Soc. 84 (2001) 230-232.
8. D. Doni Jayaseelan, N. Kondo, M.E. Brito, and T. Ohji, J. Am. Ceram. Soc. 85 (2002) 267-269.
9. D. Doni Jayaseelan, D. Amutha Rani, T. Nishikawa, and H. Awaji, J. Europ. Ceram. Soc. 22 (2002) 1113-1117.
10. R.D. Bagley, I.B. Cutler, and D.L. Johnson, 53 (1970) 136-141.
11. S.I. Bae, and S.J. Baik, J. Am. Ceram. Soc. 77 (1994) 2499-2504.
12. Y.Z. Li, C.M. Wang, H., M. Chan, J.M. Rickman, and M.P. Harmer, J. Am. Ceram. Soc. 82 (1999) 1497-1504.
13. J. Cho, C.M. Wang, H., M. Chan, J.M. Rickman, and M.P. Harmer, Acta. Mater. 47 (1999) 4197-4207.
14. L. Gao, J.S. Hong, H. Miyamoto, and S.D.D.L. Torre, J. Europ. Ceram. Soc. 20 (2000) 2149-2152.
15. S.T. Oh, K.I. Tajima, M. Ando, and T. Ohji, J. Am. Ceram. Soc. 83 (2000) 1314-1316.
16. R.W. Rice, J. Mat. Sci. 32 (1997) 4731-4736.
17. Z.Y. Deng, T. Fukusawa, M. Ando, G.J. Zhang, and T. Ohji, Acta. Mater. 49 (2001) 1939-1946.
18. F.E. Litovsky, M. Shapiro, and A. Shavit, J. Am. Ceram. Soc. 80 (1997) 2100-2104.
19. Ch. Kawai, and A. Yamakawa, J. Am. Ceram. Soc. 80 (1997) 2705-2708.
20. N. Ramakrishnan, and V.S. Arunachalam, J. Am. Ceram. Soc. 76 (1993) 2745-274.